Theoretical analysis on the mechanism and transformation kinetics under non-isothermal conditions
Application to the crystallization of the semiconducting $Sb_{0.16}As_{0.36}Se_{0.48}$ alloy

P.L. López-Alemany, J. Vázquez*, P. Villares, R. Jiménez-Garay

Departamento de Física de la Materia Condensada, Facultad de Ciencias, Universidad de Cádiz. Apartado 40, 11510 Puerto Real, Cádiz, Spain

Abstract

A procedure has been developed for analyzing the evolution with time of the volume fraction crystallized and reaction mechanism and for calculating the kinetic parameters at non-isothermal transformations in materials involving formation and growth of nuclei. Considering the assumptions of extended volume and random nucleation, a general expression of the fraction crystallized as a function of the time has been obtained in isothermal crystallization processes. The application of the crystallization rate equation to the non-isothermal processes has been carried out under the restriction of a nucleation which takes place early in the transformation and the nucleation frequency is zero thereafter. In these conditions, the correct reaction mechanism has been obtained plotting the logarithmic form of various kinetic equations versus the reciprocal temperature, and choosing that equation, which gives the plot with the best fit to a straight line. The kinetic parameters, activation energy and frequency factor, have been deduced from the slope and intercept of the above-mentioned straight line. The theoretical method developed has been applied to the crystallization kinetics of the semiconducting $Sb_{0.16}As_{0.36}Se_{0.48}$ alloy, thus obtaining values for the quoted parameters that agree very satisfactorily with the calculated results by other mathematical treatments. This fact shows the reliability of the theoretical method developed. © 2000 Elsevier Science S.A. All rights reserved.

Keywords: Glassy semiconductor; Nucleation and crystal growth; Differential scanning calorimetry; Kinetic equation; Reaction mechanism; Heating rate; Kinetic parameters

1. Introduction

The classical theory of nucleation and crystal growth has been well developed over the last 60 years. The treatment of condensed systems was adapted from the classical theory of the vapor–liquid transition by Turnbull and Fisher [1]. A full development of the theory is given by Christian [2] and a recent review published by Kelton [3]. The last decades have seen a strong theoretical and practical interest in the application of isothermal and non-isothermal experimental analysis techniques to the study of phase transformations. While isothermal experimental analysis techniques are in most cases more definitive, non-isothermal thermo-analytical techniques have several advantages. The rapidity with which non-isothermal experiments can be performed makes these types of experiments attractive. There has been an increasingly widespread use of non-isothermal techniques to study solid state transformations and to determine the kinetic pa-

rameters of the rate controlling processes. The techniques have become particularly prevalent for determination of the thermal stability of amorphous alloys and in the investigation of the processes of nucleation and growth that occur during transformation of the metastable phases in a glassy alloy as it is heated. These techniques provide rapid information on such parameters as glass transition temperature and transformation enthalpy, temperature and activation energy over a wide range of temperature [4,5]. In addition, the physical form and high thermal conductivity as well as the temperature at which transformations occur in most amorphous alloys make these transformations particularly suited to analysis in a differential scanning calorimeter (DSC). There is a large variety of theoretical models and mathematical treatments to explain the crystallization kinetics. While all of the treatment are based on the formal theory of transformation kinetics, they differ greatly in their assumptions and in some cases lead to contradictory results. It was suggested by Henderson [5] in a notable work that many of the treatments are based on an incomplete understanding of the formal theory of transformation kinetics.

* Corresponding author. Tel.: +349-56-830966; fax: +349-56-834924.
E-mail address: wagner@merlin.eca.es (J. Vázquez)

It should be noted that glass-forming liquids provide systems in which the temperature of the liquid–crystal interface is well defined by the temperature of the system, and therefore, the time evolution of the crystallization kinetics can meaningfully be measured using thermal analysis techniques. Thus, it is not surprising that recently the differential scanning calorimetry has been considered as a technique that is applicable to the study of the crystallization kinetics of glass-forming liquids [6–12]; with very few exceptions the analysis of the data obtained has been carried out using the Johnson–Mehl–Avrami (JMA) transformation rate equation.

In this work, a theoretical method has been developed for determining the volume fraction crystallized, the correct reaction mechanism and the kinetic parameters by DSC, using non-isothermal techniques in solid systems involving formation and growth of nuclei, starting from the formal theory of transformation kinetics. The quoted method has been used to analyze the crystallization kinetics of the glassy semiconducting $Sb_{0.16}As_{0.36}Se_{0.48}$ by using DSC with continuous-heating techniques.

2. Theoretical background

The crystallization is a particular case of the nucleation and grain growth controlled solid-state transformation processes, the theory of which is well-known [13–18]. If an embryo of the transformed phase nucleates at moment τ and grows thereafter anisotropically with principal growth velocities, $u_i(t')$ ($i=1, 2, 3$), in three mutually perpendicular directions, then its volume v at moment t (where $\tau < t' < t$) is

$$v(\tau, t) = g \prod_i \int_\tau^t u_i(t') \mathrm{d}t' \tag{1}$$

being g a geometric factor which depends on the shape of the growing crystal and the expression $\prod_i \int_\tau^t u_i(t') \mathrm{d}t'$ condenses the product of the integrals corresponding to the values of the above quoted subscript i.

When the possible overlap of grains is neglected, it is possible to define an extended volume of transformed material, V_e, by the relationship

$$\mathrm{d}V_e = v(\tau, t) I_v(\tau)(V_a + V_b)\mathrm{d}\tau = v(\tau, t)V I_v(\tau)\mathrm{d}\tau \tag{2}$$

where, $I_v(\tau)$ is the nucleation frequency per unity volume; V_a and V_b, the untransformed and transformed volumes, respectively, and V, the volume of whole assembly. As the change of the real transformed volume, $\mathrm{d}V_b$, and that of the extended volume, $\mathrm{d}V_e$, are related by

$$\mathrm{d}V_b = \left(1 - \frac{V_b}{V}\right)\mathrm{d}V_e = (1 - x)\mathrm{d}V_e \tag{3}$$

being $x = V_b/V$, the volume fraction transformed. Differentiating this expression and substituting the result in Eq. (3), one obtains

$$\frac{\mathrm{d}x}{1 - x} = \frac{\mathrm{d}V_e}{V} \tag{4}$$

equation, which one relates to Eq. (2), where the value for $v(\tau, t)$ from the Eq. (1) has been included, yielding

$$x(t) = 1 - \exp\left\{-g \int_0^t I_v(\tau)\left[\prod_i \int_\tau^t u_i(t')\mathrm{d}t'\right]\mathrm{d}\tau\right\} \tag{5}$$

the basic nucleation-growth equation for the transformed fraction, x.

When the crystal growth rate is isotropic, $u_i(t')=u(t')$, assumption which is in agreement with the experimental evidence, since in many transformations the reaction product grows approximately with the same rate in all directions, the Eq. (5) can be written as:

$$x(t) = 1 - \exp\left[-g \int_0^t I_v(\tau)\left(\int_\tau^t u(t')\mathrm{d}t'\right)^m \mathrm{d}\tau\right]. \tag{6}$$

Here m is an integer or half integer, which depends on the mechanism of growth and the dimensionality of the crystal.

Eq. (6) is evidently valid under any thermal conditions. Up to this point, no assumptions have been made regarding the origin of the time dependence of I_v and u, however, it should be noted an important limitation of this equation, which stems from the use of Eq. (3), which describes a completely random overlap of growing crystallites.

For the important case of isothermal crystallization with nucleation frequency and growth rate independent of time, Eq. (6) can be integrated to yield

$$x(t) = 1 - \exp(-g' I_v u^m t^n) \tag{7}$$

where $n=m+1$ for $I_v \neq 0$ and g' is a new shape factor.

Eq. (7) can be taken as a detailed specific case of the JMA [13,16] transformation equation

$$x(t) = 1 - \exp\left[-(Kt)^n\right] \tag{8}$$

In this equation, the reaction rate constant, K, is a function of temperature, and as it is proportional to $(I_v u^m)^{1/n}$, in general, depends on both the nucleation frequency and the crystal growth rate, and n is a parameter which reflects the nucleation frequency and/or growth morphology.

The isothermal transformation rate, $\mathrm{d}x(t)/\mathrm{d}t$, can be easily determined from Eq. (8) by differentiating with respect to time and substituting in resulting expression the explicit relation between x and t given by Eq. (8) to yield

$$\frac{\mathrm{d}x}{\mathrm{d}t} = nK(1 - x)\left[-\ln(1 - x)\right]^{(n-1)/n} \tag{9}$$

This equation is sometimes referred to as the JMA transformation rate equation.

2.1. Applicability of the JMA transformation rate equation under conditions of continuous heating

It should be noted that Eq. (8) and, therefore, Eq. (9) as developed by JMA are based on the following important assumptions:

1. Isothermal transformation conditions;
2. Spatially random nucleation;
3. Growth rate of new phase dependent only on temperature and not time (i.e., linear growth kinetics).

In the past decades, Eq. (9) has been applied without qualification to the analysis of non-isothermal phase transformations [19–21]. However, according to literature [22], the above-mentioned equation can only be rigorously applied to transformations involving nucleation and growth in a limited number of special cases under non-isothermal conditions. In particular, if it can be shown that the transformation rate depends only on the state variables of fraction transformed, x, and temperature, T, and not on thermal history, then Eq. (9) can be used to describe non-isothermal as well as isothermal transformations consistent with assumptions (2) and (3) above. Therefore, the criteria which are necessary in order to apply Eq. (9) to the non-isothermal crystallization process in glass forming liquids are thus restrictive. Under these restrictions, an example of a system which allows the non-isothermal application of Eq. (9) is one in which the nucleation process takes place early in the transformation and the nucleation frequency is zero thereafter. This case has been referred to as 'site saturation' in the literature [23–25]. In addition, in the cases as the above-mentioned, the reaction rate constant can be defined by a function with an Arrhenian temperature dependence, $K = K_0 \exp(-E/RT)$ [26]. In this expression of the rate constant, K_0 is the frequency factor; E, the overall effective activation energy, and R, the ideal gas constant.

2.1.1. Obtaining the correct reaction mechanism by non-isothermal techniques

In the derivation of relationships for analyzing the mechanism of the solid state transformations by using techniques of continuous heating, it is necessary as previously said, a reaction rate independent of the thermal history and expressed as the product of two separable functions of absolute temperature and the fraction transformed. In these conditions, Eq. (9) can be written as

$$\frac{\mathrm{d}x}{\mathrm{d}t} = Kf(x) = K_0 f(x) \left[\exp\left(\frac{-E}{RT}\right) \right] \tag{10}$$

where, $f(x) = n(1-x)[-\ln(1-x)]^{(n-1)/n}$ is a function which depend on the mechanism of the process.

Bearing in mind that the heating rate is $\beta = \mathrm{d}T/\mathrm{d}t$, Eq. (10) must be integrated by separation of variables and one obtains

$$g(x) = \int_0^x \frac{\mathrm{d}x'}{f(x')} = \frac{K_0}{\beta} \int_{T_0}^T \left[\exp\left(\frac{-E}{RT'}\right) \mathrm{d}T' \right] \tag{11}$$

and replacing E/RT' with y', the logarithmic form of Eq. (11) can be expressed as

$$\ln[g(x)] = \ln\frac{K_0 E}{\beta R} + \ln\left[\int_y^\infty \mathrm{e}^{-y'} y'^{-2} \mathrm{d}y' \right]$$

$$= \ln\frac{K_0 E}{\beta R} + \ln[p(y)] \tag{12}$$

if it is assumed that $T_0 \ll T$, so that y_0 can be taken as infinity. This assumption is justifiable for any heating treatment which begins at a temperature where nucleation and crystal growth are negligible, i.e., below T_g (glass transition temperature) for most glass forming systems [26].

The function $\int_y^\infty \mathrm{e}^{-y'} y'^{-2} \mathrm{d}y'$ is not integrable in closed form and the authors Vázquez et al. [27] have developed a method to evaluate it by an alternating series, resulting

$$p(y) = \left[-\frac{\mathrm{e}^{-y'}}{y'^2} \sum_{k=0}^\infty \frac{(-1)^k (k+1)!}{y'^k} \right]_y^\infty$$

$$= \frac{\mathrm{e}^{-y}}{y^2} \sum_{k=0}^\infty \frac{(-1)^k (k+1)!}{y^k}. \tag{13}$$

The expression $\ln[p(y)]$ is, to a first approximation, a linear function of $1/T$ if y is sufficiently large, therefore, in the range of values of y, $20 < y < 60$, the function $\ln[p(y)]$ with $k=0$ can be fitted very satisfactorily by a linear approximation, (see Fig. 1) giving

$$\ln(\mathrm{e}^{-y} y^{-2}) \cong -5.1202 - 1.052y. \tag{14}$$

It should be noted that the term $\ln[K_0 E(\beta R)^{-1}]$ in Eq. (12) is independent of temperature. Thus, the difference of $\ln[g(x)]$ and $\ln[p(y)]$, both functions of the temperature, does not depend upon the temperature in the whole temperature
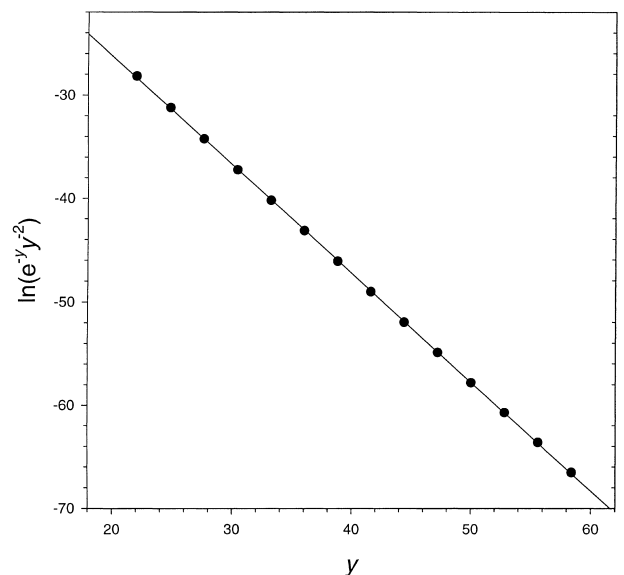

Fig. 1. Representation of $\ln(\mathrm{e}^{-y} y^{-2})$ vs. y and corresponding straight regression line for the range of values $20 < y < 60$.

Table 1
Theoretical kinetic model equations considered

Equation	$f(x)$	$g(x)$	Rate-controlling process	Label
Tamman	$(2x)^{-1}$	x^2	One-dimensional diffusion	D_1
Valensi	$[-\ln(1-x)]^{-1}$	$(1-x)\ln(1-x)+x$	Two-dimensional diffusion, cylindrical symmetry	D_2
Jander	$(3/2)(1-x)^{1/3}[(1-x)^{-1/3}-1]^{-1}$	$[1-(1-x)^{1/3}]^2$	Three-dimensional diffusion, spherical symmetry	D_3
Ginstling–Brownshtein	$(3/2)[(1-x)^{-1/3}-1]^{-1}$	$1-(2/3)x-(1-x)^{2/3}$	Three-dimensional diffusion, spherical symmetry	D_4
Jonson–Mehl–Avrami (JMA)	$n(1-x)[-\ln(1-x)]^{(n-1)/n}$	$[-\ln(1-x)]^{1/n}$	Random nucleation	A_n
Mampel unimolecular law	$1-x$	$-\ln(1-x)$	Random nucleation, one nucleus on each particle	F_1
JMA ($n=2$)	$2(1-x)[-\ln(1-x)]^{1/2}$	$[-\ln(1-x)]^{1/2}$	Random nucleation; Avrami equation I	A_2
JMA ($n=3$)	$3(1-x)[-\ln(1-x)]^{2/3}$	$[-\ln(1-x)]^{1/3}$	Random nucleation; Avrami equation II	A_3
	$2(1-x)^{1/2}$	$1-(1-x)^{1/2}$	Phase boundary reaction, cylindrical symmetry	R_2
Shrinking sphere	$3(1-x)^{2/3}$	$1-(1-x)^{1/3}$	Phase boundary reaction, spherical symmetry	R_3

interval in which the process proceeds. In addition, considering Eq. (12) and the above-mentioned fact that $\ln[p(y)]$ is a linear function of $1/T$, the relation $\ln[g(x)]$ must also be a linear function of $1/T$. For the correct mechanism $\ln[g(x)]$, thus, be linear function of $1/T$. The values of $\ln[g(x)]$ calculated for the various rate processes using DSC trace and plotted versus the corresponding $1/T$ values should give a straight line only for the rate process, which can be designated as the most probable. The others, for which this plot is not linear, can be refused. The sensitivity of this procedure for the mechanism determination is, as in all non-isothermal methods, not too high. But it yet gives valuable and useful informations. Therefore, the analysis of $f(x)$ is useful if we want to distinguish which one of the several kinetic models [28,29] can describe the crystallization process. Several kinetic equations are presented in Table 1. Some equations, labelled D, correspond to reactions controlled by diffusion through the sample. Others, labelled R, correspond to a reaction process controlled by diffusion across the interface. The consideration of a nucleation process prior to crystal growth is taken into account in other kinetic models labelled A. The curves of Fig. 2 are the plots of $\ln[g(x)]$ versus $1/T$ being calculated from DSC trace of the $Sb_{0.16}As_{0.36}Se_{0.48}$ glassy alloy for $\beta=8\,K\,min^{-1}$ employing the different kinetic equations given in Table 1. A set of values for the magnitudes T and x in the intervals 536.2–579.9 K and 0.08–0.96 K, respectively, has been chosen for the above-mentioned plots. It should be noted that only the plot for $\ln[-\ln(1-x)]$ (F_1) gives a good straight line (correlation coefficient $r^2=0.999$). The other equations can be refused. Deviations from the linearity are comparatively very small in the case of the labelled equations A_2 and A_3. The other informations about the process studied are evidently required for the correct decision concerning the choice of the true mechanism for the process investigated.

2.1.2. Calculating the kinetic parameters by using the $p(y)$ function

The function $p(y)$ is obtained, as previously said, by integration of the temperature dependent reaction rate constant within a temperature interval from T_0 to $T(T_0 \ll T)$ and is

expressed by the series of Eq. (13). For the correct reaction mechanism, and according to Eq. (12), the linear plots of $\ln[g(x)]$ versus $1/T$ and $\ln[p(y)]$ versus $1/T$ have the same slope, which can be designated as $\tan\alpha$, yielding

$$\tan\alpha = \frac{d\{\ln[p(y)]\}}{d(1/T)} = \frac{E}{R}\frac{d\{\ln[p(y)]\}}{dy} \tag{15}$$

Taking the derivative of logarithmic form of Eq. (13) with respect to y, one obtains

$$\begin{aligned}
\frac{d\{\ln[p(y)]\}}{dy} &= -1 - 2y^{-1} \\
&\quad + \left[\sum_{k=0}^{\infty}\frac{(-1)^k(k+1)(k+2)!}{y^{k+2}}\right]\left[\sum_{k=0}^{\infty}\frac{(-1)^k(k+1)!}{y^k}\right]^{-1} \\
&= -\left[\sum_{k=0}^{\infty}\frac{(-1)^k(k+1)!}{y^k}\right]^{-1} \tag{16}
\end{aligned}$$

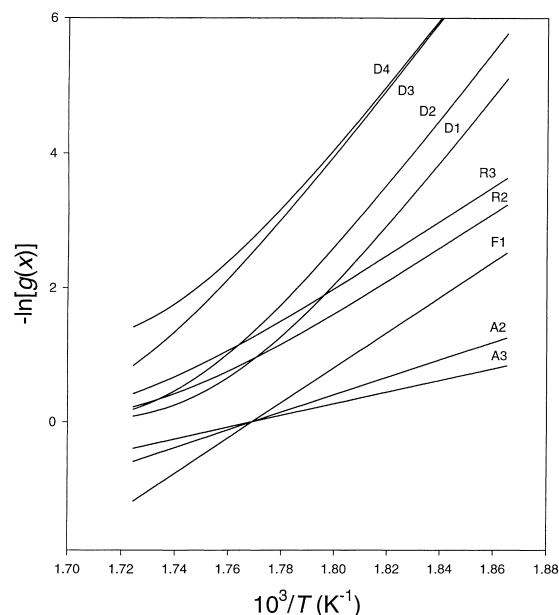Fig. 2. Plots of $\ln[g(x)]$ vs. $1/T$ calculated from the DSC trace of the $Sb_{0.16}As_{0.36}Se_{0.48}$ glassy alloy for $\beta=8\,K\,min^{-1}$ and using the different kinetic equations given in Table 1.

and introducing Eq. (13) into Eq. (16), the slope of $\ln[p(y)]$ versus $1/T$ is then

$$\tan\alpha = -\frac{E}{R}\frac{1}{y^2 e^y p(y)} = -\frac{E}{R}\left[\sum_{k=0}^{\infty}\frac{(-1)^k (k+1)!}{y^k}\right]^{-1}. \quad (17)$$

For large values of y, it is possible to use only the two first terms of the above series, without making any appreciable error and thus the activation energy can be calculated approximately from the equation

$$E \cong \frac{R}{2}\left(-\tan\alpha + \sqrt{\tan^2\alpha + 8\bar{T}\tan\alpha}\right) \quad (18)$$

being $\bar{T}$ the mean temperature. The value of E can be found easy by a comparison of the slope of the straight line of $\ln[g(x)]$ versus $1/T$ with a set of the lines of $\ln[p(y)]$ versus $1/T$ (Fig. 3) constructed for the different values of E. The slope of both functions should be the same in the temperature interval in which the process proceeds.

In addition, substituting the linear approximation of $\ln[p(y)]$ (Eq. (14)) into Eq. (12) results

$$\ln[g(x)] = \ln\frac{K_0 E}{\beta R} - 5.1202 - 1.052\frac{E}{RT} \quad (19)$$

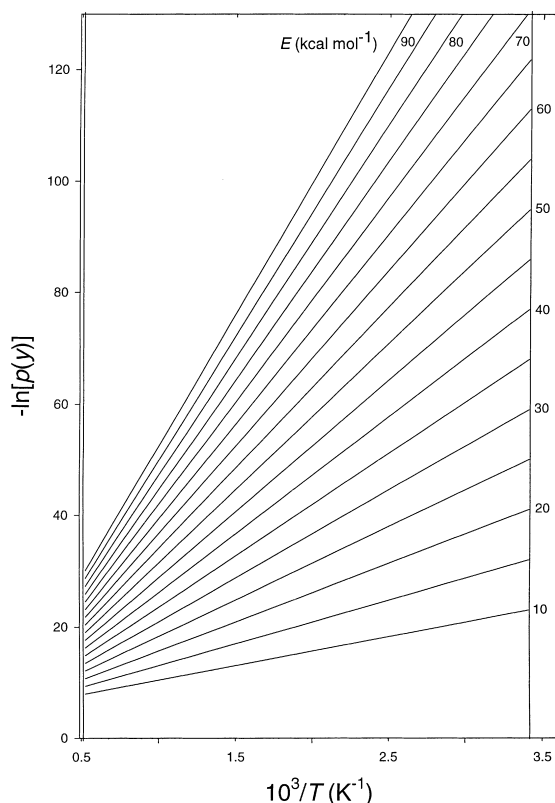the equation of a straight line, the intercept of which gives the frequency factor, K_0.

Fig. 3. Plots of $-\ln[p(y)]$ vs. $1/T$ for various activation energies, E.

On the other hand, in order to establish the range of the validity of the above mentioned linear approximation the well-know Taylor expansion can be put to use:

$$\ln[p(y)] = \ln[p(y_1)] + (y - y_1)\left.\frac{d\{\ln[p(y)]\}}{dy}\right|_{y=y_1}$$
$$+ \frac{(y-y_1)^2}{2}\left.\frac{d^2\{\ln[p(y)]\}}{dy^2}\right|_{y=y_1} + \dots \quad (20)$$

where y_1 is the chosen point of the approximation. Neglecting terms of the exponent above two in Eq. (20), after substitution

$$\ln[p(y)] = \ln[p(y_1)] + A(y_1)(y - y_1) + \tfrac{1}{2}B(y_1)(y - y_1)^2 \quad (21)$$

where $A(y_1) = -\left[y_1^2 e^{y_1} p(y_1)\right]^{-1}$ has been obtained from Eqs. (16) and (13) and

$$B(y_1) = \left\{\frac{d}{dy}\left[-y^{-2}e^{-y}[p(y)]^{-1}\right]\right\}\Big|_{y=y_1}$$
$$= \left\{e^{-y}y^{-2}[p(y)]^{-1}\left[\frac{y+2}{y}\right.\right.$$
$$\left.\left.+ [p(y)]^{-1}\frac{dp(y)}{dy}\right]\right\}\Big|_{y=y_1}$$
$$= -\frac{y_1+2}{y_1}A(y_1) - A^2(y_1).$$

In practice, the graphical comparison of the linear with the parabolic substitution in Eq. (21) gives evidence for the validity range of the linear approximation. Table 2 provides data of $\ln[p(y_1)]$ and the coefficients $A(y_1)$ and $B(y_1)/2$. The most unfavourable case, $y_1=10$, is illustrated diagrammatically in Fig. 4 with regard to $(y-y_1)$ in Eq. (21). Bearing in mind the relationship $(E/RT)-(E/RT_1)=y-y_1$ and defining $\Delta T=T-T_1$, one obtains

$$\Delta T = \pm\left|\frac{-RT_1^2(y - y_1)}{E + RT_1(y - y_1)}\right|$$

This expression has allowed to obtain the ΔT-values, shown in Fig. 4, from the activation energies and temperatures also given in Fig. 4. It is easily seen that the parabolic term has a negligible influence for $(y-y_1)$ below about one, since only represents the 0.2% of the overall value of the $\ln[p(y)]$. This fact means that for a normal temperature interval within about 100 K the straight line is really an excellent approximation. Therefore, the value of the activation energy can be

Table 2
Values of $\ln[p(y_1)]$ and of the coefficients $A(y_1)$ and $(1/2)B(y_1)$

Quantity	Values				
y_1	10	20	30	40	50
$-\ln[p(y_1)]$	14.7	26.1	36.8	47.4	57.8
$-A(y_1)$	1.163	1.093	1.064	1.049	1.039
$(1/2)B(y_1)$	2.2×10^{-2}	3.8×10^{-3}	1.4×10^{-3}	5×10^{-4}	5×10^{-4}
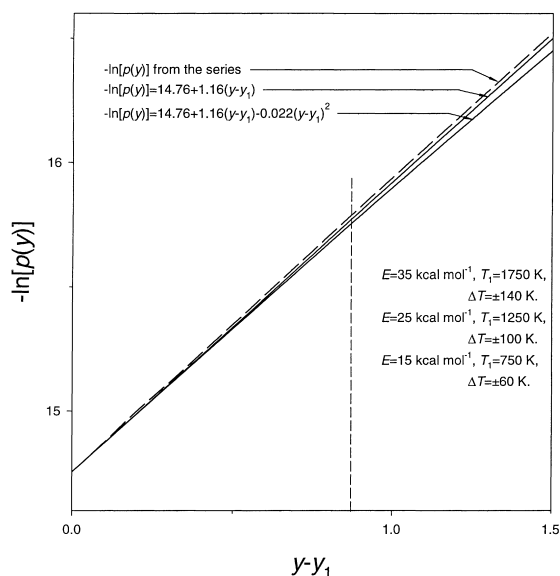
Fig. 4. Graphical comparison of the linear with the parabolic substitution in Eq. (21).

Fig. 5. Typical DSC trace of $Sb_{0.16}As_{0.36}Se_{0.48}$ glassy alloy at a heating rate of $32\,K\,min^{-1}$. The hatched area shows A_T the area between T_i and T.

easily obtained, equalling the slope, $\langle A(y_1)\rangle ER^{-1}$, of the linear approximation of $\ln[p(y)]$ with that of the experimental $\ln[g(x)]$ versus $1/T$ plot. It should be noted that the E-values thus obtained and those calculated from Eq. (18) compare well, and also with the ones obtained by conventional methods [26,27].

3. Experimental procedures

High purity (99.999%) antimony, arsenic and selenium in appropriate percent proportions were weighed into a quartz glass ampoule (6 mm diameter). The contents of the ampoules (7 g total) were sealed in a pressure of $10^{-2}\,N\,m^{-2}$ and heated in a rotating furnace at around 1225 K for 24 h, submitted to a longitudinal rotation of 1/3 rev min^{-1} in order to ensure the homogeneity of the molten material. It was then immersed in a receptacle containing water in order to solidify the material quickly, avoiding crystallization of the compound. The amorphous nature of the material was checked through a diffractometric X-ray scan, in a Siemens D500 diffractometer. The thermal behavior was investigated using a Perkin–Elmer DSC7 differential scanning calorimeter with an accuracy of ±0.1 K. Temperature and energy calibrations of the instrument were performed, for each heating rate, using the well-known melting temperatures and melting enthalpies of high-purity zinc and indium supplied with the instrument. Powdered samples weighing about 20 mg (particles size around 40 µm) were crimped in aluminium pans and scanned at room temperature through their glass transition temperature, T_g, at different heating rates: 1, 2, 4, 8, 16, 32 and 64 K min^{-1}. An empty aluminium pan was used as reference and in all cases a constant flow of nitrogen was maintained in order to extract the gases emitted by the
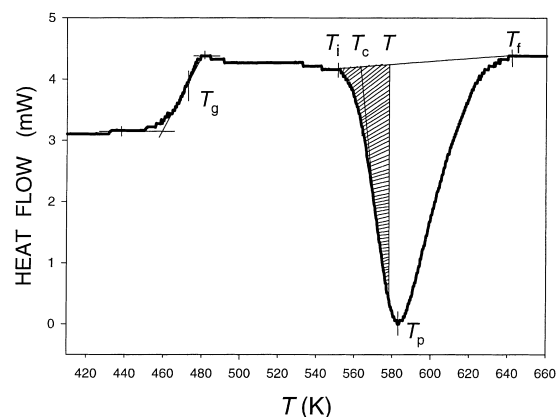
reaction, which are highly corrosive to the sensory equipment installed in the DSC furnace. The glass transition temperature was considered as a temperature corresponding to the inflection point of the lambda-like on the DSC scan, as shown in Fig. 5.

The crystallized fraction, x, at any temperature, T, is given as $x=A_T/A$, where A is the total area of the exotherm between the temperature T_i where the crystallization is just beginning and the temperature T_f where the crystallization is completed and A_T is the area between the initial temperature and a generic temperature, see Fig. 5.

4. Results and discussion

The typical DSC trace of $Sb_{0.16}As_{0.36}Se_{0.48}$ chalcogenide glass obtained at a heating rate of $32\,K\,min^{-1}$ and plotted in Fig. 5 shows three characteristic phenomena which are resolved in the temperature region studied. The first (T=474.2 K) corresponds to the glass transition temperature, T_g, the second (T=562.1 K) to the extrapolated onset crystallization temperature, T_c, and the third (T=583.7 K) to the peak temperature of crystallization T_p of the above mentioned chalcogenide glass. This behavior is typical for a glass-crystalline transformation. The temperature values T_g, T_c and T_p increase with increasing heating rate. The area under the DSC curve is directly proportional to the total amount of alloy crystallized. The ratio between the ordinates and the total area of the peak gives the corresponding crystallization rates, which makes it possible to plot the curves of the exothermal peaks represented in Fig. 6. It may be observed that the $(dx/dt)_p$ values increase in the same proportion as the heating rate, a property which has been widely discussed in the literature [30,31].

With the aim of analyzing the crystallization kinetics of the glassy alloy $Sb_{0.16}As_{0.36}Se_{0.48}$, the values of the magnitudes described by the thermograms for the different heating rates, quoted in Section 3, are obtained and
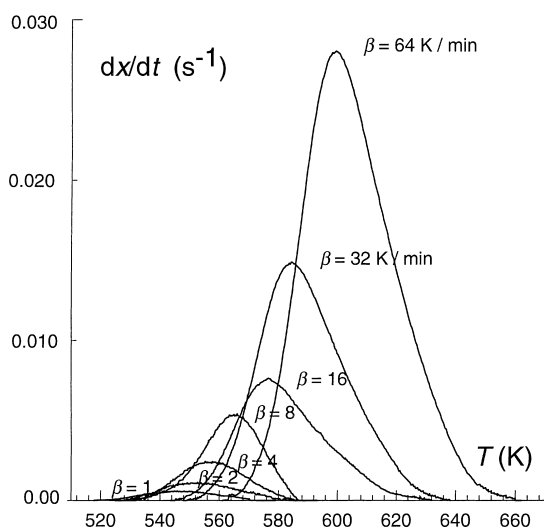
Fig. 6. Crystallization rate versus temperature of the exothermal peaks at different heating rates.

given in Table 3. The crystallization mechanism has been analyzed and kinetic parameters have been calculated, according to the preceding theory. Thus, for a heating rate of $8 \, \mathrm{K \, min^{-1}}$, it has been found that the kinetic equation $g(x)=-\ln(1-x)=Kt$ (a JMA transformation equation with $n=1$) gives the best fit to a straight line. Therefore, the above-mentioned mechanism can be described by means a process of random nucleation with one nucleus on each particle, i.e. the kinetic exponent $n=1$. From the above mentioned fit, the following equation is obtained

$$\ln[-\ln(1-x)] = -26124.14 \, T^{-1} + 46.21$$
$$= -T^{-1}\tan\alpha + 46.21 \tag{22}$$

whose slope together with $\overline{T}=558.0 \, \mathrm{K}$, the mean value of the temperature in the interval 536.2–579.9 K, have been substituted into Eq. (18), resulting the activation energy of the process, $E=49.9 \, \mathrm{kcal \, mol^{-1}}$. The intercepts of Eqs. (19) and (22) have been equated to obtain the frequency factor $K_0=1.1\times10^{17} \, \mathrm{s^{-1}}$

Also the activation energy has been calculated equalling the slope of Eq. (22) with the expression $\langle A(y_1)\rangle ER^{-1}$,

Table 3
Experimental data obtained from the thermograms corresponding to the crystallization process of alloys $Sb_{0.16}As_{0.36}Se_{0.48}$

β (K min^{-1})	T_g (K)	T_i (K)	T_p (K)	$10^3 \times (dx/dt)_p$ (s^{-1})
1	456.4	518.0	545.0	0.487
2	461.0	524.9	549.5	0.974
4	462.4	528.9	555.3	1.988
8	467.1	529.6	564.9	4.112
16	470.9	549.0	574.3	8.227
32	474.2	554.1	583.7	16.454
64	480.2	571.3	598.4	31.542

quoted in Section 2.1.2 and taking for $\langle A(y_1)\rangle$ the mean value of the corresponding data in Table 2. A value of $48.3 \, \mathrm{kcal \, mol^{-1}}$ for above-mentioned energy has been obtained. It should be noted that the E-values calculated by the two forms described compare well, since only differ a 3.2%.

Trying to confirm the reliability of the theoretical method described the kinetic parameters E, n and K_0 have been also obtained, in the work, from other mathematical treatments, quoted in the literature [5,30,32–35].

As an example, the values of the above-mentioned parameters, calculated by Kissinger method [33,34] are presented. By using the linear relationship

$$\ln\left(\frac{T_p^2}{\beta}\right) = \frac{E}{RT_p} - \ln\left(\frac{K_0 R}{E}\right)$$

it is possible to obtain both the overall effective activation energy and the frequency factor of the crystallization process.

From the experimental data, a plot of $\ln(T_p^2/\beta)$ versus $1/T_p$ has been drawn at each heating rate and also the straight regression line shown in Fig. 7. From the slope and the intercept of the experimental straight line the values of the activation energy, $E=47.2 \, \mathrm{kcal \, mol^{-1}}$, and frequency factor, $K_0=1.2\times10^{16} \, \mathrm{s^{-1}}$, respectively, has been deduced.

In addition, the experimental data T_p and $(dx/dt)_p$ (Table 3), which correspond to the maximum crystallization rate for each heating rate, and the above-mentioned value of the activation energy, make it possible to determine, through relationship

$$n = RT_p^2 \left.\frac{dx}{dt}\right|_p (0.37\beta E)^{-1},$$

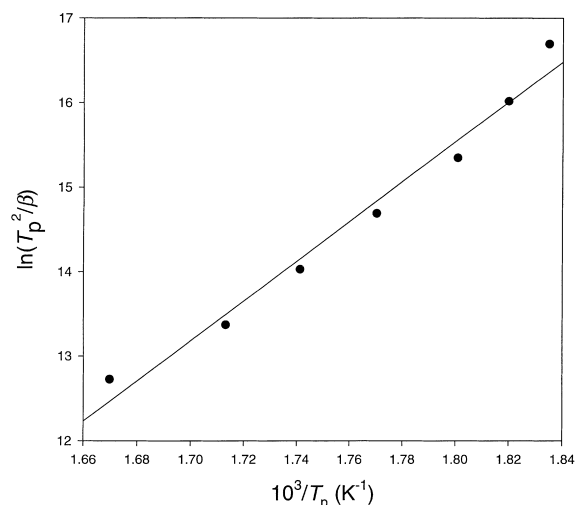the kinetic exponent for each the experimental heating rates, whose mean value is $\langle n \rangle = 1.1$.

Fig. 7. Experimental plots of $\ln(T_p^2/\beta)$ vs. $10^3/T_p$ and straight regression line of $Sb_{0.16}As_{0.36}Se_{0.48}$ alloy (β in K s^{-1}).

These results agree very satisfactorily with the theoretical values obtained by means of the developed method, confirming the reliability of the above-mentioned method.

From the obtained values for the kinetic parameters and according to the Avrami theory [14–16] of nucleation, the relatively high value found for the pre-exponential factor (frequency factor related to the probability of molecular collisions) seems to confirm the fact that in the crystallization reaction mechanism there is a random nucleation, coherent with the basic formalism used. Bearing in mind the usual criteria for the interpretation of kinetic exponent [2,36], some observations relating to the morphology of the growth can be worked out. In the glassy alloy $Sb_{0.16}As_{0.36}Se_{0.48}$, there is a relatively stable crystallization phase ($E=49.9\,\text{kcal mol}^{-1}$), exhibiting a bulk nucleation, and according to the literature [2] the crystalline phase may exhibit a growth of 'needles and plates of finite long dimensions small in comparison with their separation', since the value of kinetic exponent is $n=1$.

5. Conclusions

The described theoretical procedure enable us to study the evolution with time of the volume fraction transformed in materials involving nucleation and crystal growth processes. This method assumes the concept of the extended volume in transformed material and the condition of random nucleation. Using these assumptions has been obtained a general expression s for the transformed fraction, as a function of the time in bulk crystallization processes. In the case of isothermal crystallization, the above-mentioned expression has been transformed in an equation, which can be taken as a specific case of the JMA transformation equation. The application of this equation to non-isothermal transformations implies restrictive conditions, as it is the case of a transformation rate, which depends only on the fraction transformed and the temperature. Under this restriction, the correct reaction mechanism is obtained plotting the logarithmic form of various kinetic equations (functions of the transformed fraction) versus the reciprocal temperature, and choosing that equation, which gives the plot with the best fit to a straight line. In addition, the integration of the reaction rate gives a temperature integral, which has been evaluated by an alternating series. The linear plots of the logarithmic form of the sum of this series versus $1/T$ and that of the kinetic equation versus $1/T$, for the correct mechanism, have the same slope, which allows to calculate the activation energy of the process. Finally, the frequency factor is obtained from the intercept of the linear plot of the logarithmic form of the kinetic equation versus $1/T$.

The theoretical method developed has been applied to the experimental data corresponding to the $Sb_{0.16}As_{0.36}Se_{0.48}$ glassy alloy. The theoretical results obtained for the kinetic parameters agree very satisfactorily with the calculated values by other mathematical treatments, confirming the reliability of the method described.

References

[1] D. Turnbull, J.C. Fisher, J. Chem. Phys. 17 (1949) 71.
[2] J.W. Christian, The Theory of Transformations in Metals and Alloys, 2nd Edition, Pergamon Press, New York, 1975.
[3] K.F. Kelton, Crystal Nucleation in Liquids and Glasses, Solid State Physics, Vol. 45, Academic Press, New York, 1991.
[4] Z. Altounian, J.O. Strom-Olsen, in: R.D. Shull, A. Joshi (Eds.), Thermal Analysis in Metallurgy, The Minerals, Metals and Materials Society, Warrendale, PA, 1992, p. 155.
[5] D.W. Henderson, J. Non-Cryst. Solids 30 (1979) 301.
[6] D.D. Thornburg, R.I. Johnson, J. Non-Cryst. Solids 17 (1975) 2.
[7] N. Clavaguera, J. Non-Cryst. Solids 22 (1976) 23.
[8] H.S. Chen, J. Non-Cryst. Solids 27 (1978) 257.
[9] J. Vázquez, R.A. Ligero, P. Villares, R. Jiménez-Garay, Thermochim. Acta 157 (1990) 181.
[10] R.A. Ligero, J. Vázquez, P. Villares, R. Jiménez-Garay, J. Mater. Sci. 26 (1991) 211.
[11] R.A. Ligero, M. Casas-Ruiz, J. Vázquez, R. Jiménez-Garay, Phys. Chem. Glasses 34 (1993) 12.
[12] C. Wagner, J. Vázquez, P. Villares, R. Jiménez-Garay, Mater. Chem. Phys. 38 (1994) 74.
[13] W.A. Johnson, K.F. Mehl, Trans. Am. Inst. Mining. Met. Eng. 135 (1939) 416.
[14] M. Avrami, J. Chem. Phys. 7 (1939) 1103.
[15] M. Avrami, J. Chem. Phys. 8 (1940) 212.
[16] M. Avrami, J. Chem. Phys. 9 (1941) 177.
[17] A.N. Kolmogorov, Izv. Akad. Nauk USSR Ser. Math. 1 (1937) 355.
[18] B.V. Erofeev, N.I. Mitzkevich, in: Reactivity of Solids, Elsevier, Amsterdam, 1961, p. 273.
[19] F. Skvara, V. Satava, J. Therm. Anal. 2 (1970) 325.
[20] J. Sestak, Thermochim. Acta 3 (1971) 1.
[21] J. Sestak, Phys. Chem. Glasses 6 (1974) 137.
[22] T. Kemény, Thermochim. Acta 110 (1987) 131.
[23] J.W. Cahn, Acta Met. 4 (1956) 449.
[24] J.W. Cahn, Acta Met. 4 (1956) 573.
[25] J. Vázquez, P.L. López-Alemany, P. Villares, R. Jiménez-Garay, Thermochim. Acta 327 (1999) 191.
[26] H. Yinnon, D.R. Uhlmann, J. Non-Cryst. Solids 54 (1983) 253.
[27] J. Vázquez, C. Wagner, P. Villares, R. Jiménez-Garay, Acta Mater. 44 (1996) 4807.
[28] M.E. Brown, A.K. Galwey, Thermochim. Acta 29 (1979) 129.
[29] S.F. Hulbert, J. Br. Ceram. Soc. 6 (1969) 11.
[30] Y.Q. Gao, W. Wang, F.Q. Zheng, X. Liu, J. Non-Cryst. Solids 81 (1986) 135.
[31] J. Vázquez, P.L. López-Alemany, P. Villares, R. Jiménez-Garay, Mater. Chem. Phys. 57 (1998) 162.
[32] J.A. Augis, J.E. Bennett, J. Therm. Anal. 13 (1978) 283.
[33] H.E. Kissinger, Anal. Chem. 29 (1957) 1702.
[34] J. Vázquez, P.L. López-Alemany, P. Villares, R. Jiménez-Garay, J. Alloys Comp. 270 (1998) 179.
[35] J. Vázquez, C. Wagner, P. Villares, R. Jiménez-Garay, Mater. Chem. Phys. 58 (1999) 187.
[36] C.N. Rao, K.J. Rao, Phase Transition in Solids, McGraw-Hill, New York, 1978.